Parameter Estimation for a Mathematical Model of the Cell Cycle in Frog Eggs

Jason W. Zwolak*[1], John J. Tyson[2], and Layne T. Watson[3]

Short title: Parameter Estimation in Cell Cycle Models

Keywords: cyclin-dependent kinase, M-phase promoting factor, orthogonal distance regression, Levenberg-Marquardt method

---

*[1] Department of Computer Science, Virginia Tech, Blacksburg VA 24061-0106, USA, (540) 231-5958, jzwolak@vt.edu

[2] Department of Biology, Virginia Tech, Blacksburg VA 24061-0406, USA, (540) 231-4662, tyson@vt.edu

[3] Departments of Computer Science and Mathematics, Virginia Tech, Blacksburg VA 24061-0106, USA, (540) 231-7540, ltw@cs.vt.edu

ABSTRACT

Parameter values for a kinetic model of the nuclear replication-division cycle in frog eggs are estimated by fitting solutions of the kinetic equations (nonlinear ordinary differential equations) to a suite of experimental observations. A set of optimal parameter values is found by minimizing an objective function defined as the orthogonal distance between the data and the model. The differential equations are solved by LSODAR and the objective function is minimized by ODRPACK. The optimal parameter values are close to the "guesstimates" of the modelers who first studied this problem. These tools are sufficiently general to attack more complicated problems, where guesstimation is impractical or unreliable.

1. INTRODUCTION

The ultimate goal of molecular cell biology is to understand how the information stored in the genome is read out and put into action as the physiological behavior of a living cell. At one end of this continuum, genes direct the synthesis of polypeptide chains, and at the other end, networks of interacting proteins govern how a cell moves, feeds, responds, and reproduces. We are interested in the 'last step' of computational molecular biology: to derive the physiological properties of a cell from the wiring diagrams of its underlying molecular regulatory circuits (Tyson et al., 2001). The processes we study are DNA synthesis and nuclear division, and the approach we take is deterministic modeling of the regulatory system by ordinary differential equations (ODEs). This approach provides direct, quantitative connections between mechanistic details and observable cellular behavior, but it is constrained by the difficulty of assigning numerical values to the many kinetic parameters (rate constants and binding constants) that appear in the governing differential equations. In this paper, we show how to assign 'optimal' values to the kinetic parameters in a model of the nuclear replication-division cycle in frog egg extracts. The algorithms we employ are sufficiently powerful and general to attack more challenging and important problems of cell cycle modeling in the future.

The cell cycle is the sequence of events by which a cell replicates all its components and divides them between two daughter cells, so that each daughter has the information and machinery necessary to repeat the process (Murray and Hunt, 1993). The most important component is the genome, which must be accurately replicated during interphase (each chromosome becoming two identical sister chromatids) and carefully partitioned during mitosis (sister chromatids moving to opposite poles of the mitotic spindle). These basic events, DNA synthesis and mitosis, are triggered in alternating fashion by a complex network of molecular interactions involving cyclin-dependent protein kinases (Cdk). The first 10–12 mitotic cycles of a fertilized egg provide a favorite experimental system for studying this biochemical network because the cycles of DNA synthesis (S phase) and mitosis (M phase) proceed rapidly, without the intervening gaps (G1 and G2) so characteristic of somatic cell cycles. Furthermore, for eggs of the African clawed frog, *Xenopus laevis*, protocols have been developed for making cell-free extracts that carry out DNA synthesis and nuclear division in a colloidal suspension unhindered by cell membranes.

Twenty-five years of careful biochemical studies have revealed a relatively simple control system for the nuclear division cycle in frog egg extracts (Fig. 1), which is only a subset of the reaction network in intact cells. Novak and Tyson (1993)published a thorough theoretical study of the mechanism, comparing it mostly to qualitative observations of mitotic cycles in egg extracts. At the time, Novak and Tyson postulated a set of rate constants that gave a reasonable, semi-quantitative fit of the model to experimental data. Marlovits et al. (1998) re-evaluated the model in light of more quantitative studies on MPF activation in frog egg extracts. By back-of-an-envelope calculations on the available kinetic data, they proposed a refined parameter set, not too much different from the original guesses of Novak and Tyson.

In this paper we present the frog-egg model and the experimental data in full quantitative detail, and take on the challenge of finding the parameter set that optimally fits the model to the data. We pose this problem as a test case for parameter optimization in the context of dynamic models of biochemical regulatory circuits. (In a later paper, we will pose a much more challenging problem of fitting a model of the yeast cell cycle to a broad spectrum of experimental observations.) In principle, this parameter optimization problem could be attacked by many different methods—local or global, deterministic or nondeterministic. We use an algorithm (Levenberg-Marquardt) for local, gradient-based optimization—the best currently known deterministic local optimization algorithm for nonlinear least-squares problems. Using Marlovits et al. (1998) for an initial parameter set, we show that the Levenberg-Marquardt algorithm converges quickly to a (locally) optimal parameter set not too far away, and the regression error is significantly improved. We also characterize the basin of attraction near this optimal solution. In a later paper, we will report on a global deterministic search of the parameter space of this problem. We conclude by discussing the applicability of these techniques to more complicated models.

2. MODEL

The reaction network in Fig. 1 can be converted into a set of ODEs for the time rates of change of concentrations of all the proteins in the mechanism. Before doing so, we make a number of simplifications to the mechanism. All the experiments analyzed in this paper are carried out in extracts supplemented with cycloheximide, an inhibitor of protein synthesis. Hence the extract does not synthesize cyclin from its own store of cyclin mRNA, so we set $k_1 = 0$ and ignore this reaction. The experimenter adds to the extract a known amount of exogenously produced cyclin. In all cases, the added cyclin protein has been genetically engineered to be resistant to cyclosome-mediated degradation. Hence $k_2 = 0$, and we can ignore all the degradation steps in the mechanism. Because cyclin is neither synthesized nor destroyed, the total concentration of cyclin protein in the extract is constant:

$$[\text{monomeric cyclin}] + [\text{MPF}] + [\text{preMPF}] = [\text{total cyclin}] = \text{constant},$$

where MPF is the active Cdk1:cyclin dimer and preMPF refers to the phosphorylated (low activity) form of the dimer. Next, we make the assumptions (well supported by experiment) that (1) the binding of cyclin monomers and Cdk1 monomers is very fast (k_3 is large) and (2) [total Cdk1] > [total cyclin]. Hence [monomeric cyclin] << [total cyclin], and the conservation condition on cyclin subunits becomes

$$[\text{MPF}] + [\text{preMPF}] = [\text{total cyclin}].$$

With these simplifications and assumptions, the mechanism in Fig. 1 can be described by three ODEs

$$\frac{dM}{dt} = \big(v_d'(1-D) + v_d''D\big)(C_T - M) - \big(v_w'(1-W) + v_w''W\big)M, \tag{1}$$

$$\frac{dD}{dt} = v_d\left(\frac{M(1-D)}{K_{md} + (1-D)} - \frac{\rho_d D}{K_{mdr} + D}\right), \tag{2}$$

$$\frac{dW}{dt} = v_w\left(-\frac{MW}{K_{mw} + W} + \frac{\rho_w(1-W)}{K_{mwr} + (1-W)}\right), \tag{3}$$

where

$$\begin{aligned} M &= [\text{MPF}]/[\text{total Cdk1}], \\ D &= [\text{Cdc25P}]/[\text{total Cdc25}], \\ W &= [\text{Wee1}]/[\text{total Wee1}], \\ C_T &= [\text{total cyclin}]/[\text{total Cdk1}]. \end{aligned}$$

In Eqs. (1)–(3), time is expressed in minutes, and all concentrations are dimensionless numbers, having been scaled relative to some appropriate reference concentration. In frog egg extracts, [Cdk1] is typically close to 100 nM (Solomon et al., 1990; Wei et al., 2002). Total concentrations for Cdc25, Wee1 and PPase are unknown, so we set each to 1 AU ("arbitrary unit"). All vs are pseudo-first-order rate constants (units = time^{-1}). All Ks are dimensionless Michaelis constants, i.e., ratios of true Michaelis constants ($\hat{K}$, units = concentration) to reference concentrations. The ρs are dimensionless numbers expressing the activity of the phosphatase (PPase, in Fig. 1) relative to MPF. The rate constants refer to the following reactions:

v'_d — dephosphorylation of preMPF by Cdc25 in its less-active form,
v''_d — dephosphorylation of preMPF by Cdc25 in its more-active form,
v'_w — phosphorylation of MPF by Wee1 in its less-active form,
v''_w — phosphorylation of MPF by Wee1 in its more-active form,
v_d — phosphorylation of Cdc25 by MPF,
$v_d\rho_d$ — dephosphorylation of Cdc25 by PPase,
v_w — phosphorylation of Wee1 by MPF,
$v_w\rho_w$ — dephosphorylation of Wee1 by PPase.

Table 1 indicates how the parameters in Eqs. (1)–(3), the vs and Ks without hats, are related to the fundamental kinetic parameters, the $\hat{v}$s and $\hat{K}$s, and a "dilution factor" μ. This dilution factor must be included in our calculations, because in some experiments a buffered solution of proteins is added to the frog egg extract, increasing the volume of the extract and thereby diluting all the endogenous proteins in the extract. Dilution changes the values of the scaled parameters from one experiment to the next, and must be taken into account when trying to fit the model to real data.

3. EXPERIMENTS

Our goal is to obtain the "best" estimates of the rate constants in Table 1 from the experimental data presented in Fig. 2. The figure also presents the best-fitting curves derived from ODEs (1)–(3), and the optimal parameter values (Table 2). In Table 3 we describe how each experiment is to be simulated by the model equations (1)–(3).

Experiments A–H in Fig. 2 are straightforward measurements of enzyme activity as functions of time. The data in Figs. 2I and 2J are more indirect and require further explanation.

A fundamental proposal of the Novak and Tyson (1993)model of MPF oscillations in frog egg extracts is that the processes of MPF activation (dephosphorylation of preMPF by Cdc25) and MPF inactivation (phosphorylation of MPF by Wee1) are jump transitions on a hysteresis loop. To see this, we solve Eqs. (1)–(3) for the steady-state (ss) concentrations of MPF, Cdc25, and Wee1, and plot M_{ss} as a function of C_T (total cyclin added to the extract, a parameter easily controlled by the experimentalist). The graph (Fig. 3), called a one-parameter bifurcation diagram, shows that, for $C_I < C_T < C_A$, the MPF control system exhibits bistability: two stable steady states (nodes) separated by an unstable steady state (a saddle point). One node has low MPF activity (most Cdk1:cyclin dimers are in the less active, phosphorylated form) and the other node has high MPF activity. The low-activity state corresponds to 'interphase' (when DNA is being replicated) and the high-activity state corresponds to 'mitosis' (when chromosomes are aligned on the mitotic spindle and then sister chromatids are separated). At the limits of the bistable region, the stable steady states are annihilated by coalescence with the unstable steady state (called a 'saddle-node' bifurcation).

In a classic experiment, Solomon et al. (1990) prepared an egg extract in interphase (no endogenous cyclin) and supplemented it with exogenous, non-degradable cyclin. They found that if $C_T < C_A$, then the extract remains in interphase, with little detectable MPF activity. However, if $C_T > C_A$, then the extract will eventually enter mitosis (after a time lag), and the amount of MPF activity generated by the extract will increase with increasing C_T. These observations are consistent with the theoretical picture in Fig. 3.

Novak and Tyson drew two further conclusions from Fig. 3. (1) As C_T is lowered toward the threshold ($C_T \to C_A^+$), the time lag before MPF activation should increase abruptly. (2) There should be a different threshold C_I for MPF inactivation in extracts that are transiting from mitosis back to interphase ($C_T = C_I$ for the inactivation threshold in Fig. 3). The inactivation threshold can be measured by supplementing an interphase extract with a combination of exogenously produced, degradable and nondegradable cyclins. Let C_T be the total concentration of added cyclin and f be the fraction that is nondegradable. If $C_T > C_A$, then the extract will enter mitosis, activate cyclosomes, and destroy the degradable fraction of cyclins. If the amount of cyclin remaining (fC_T) is greater than the inactivation threshold (C_I) then the extract will remain in mitosis. But if $fC_T < C_I$, then the extract will exit mitosis and return to interphase.

In a series of experiments that were never published, Jonathan Moore tested these two predictions of the Novak-Tyson model, and his results are presented in Figs. 2I and 2J. Fig. 2I shows the time lag for MPF activation, which clearly increases as C_T decreases. Fig. 2J represents the thresholds for MPF activation and inactivation. Moore's observations placed the activation threshold C_A between 0.15 and 0.20 and the inactivation threshold C_I about three-fold lower (0.06).

4. METHODS

We use the public domain software package ODRPACK to estimate the parameters of our model by minimizing the weighted sum of orthogonal distances between the experimental data and the predictions of the model. The model equations are integrated by LSODAR, a public domain software package that efficiently solves stiff and nonstiff systems of ODEs.

4.1. ODRPACK

In general, a model predicts the values of dependent variables (y) from independent variables (x) and parameter values (β):

$$y_i = f_i(x_i; \beta), i = 1 \ldots n,$$

where y, x, and β are (in general) all vectors and f_i is the model for the ith datum. Suppose the experimental data can be expressed by vectors y_i and x_i, $i = 1, \ldots, n$. If the model fits the data perfectly, for a specific parameter vector $\hat{\beta}$, then $y_i = f_i(x_i; \hat{\beta})$ for all i. It is always the case that there are discrepancies between the model and observations because of errors in the measurements and/or inadequacies of the model. ODRPACK constructs an objective function that is a scalar measure of the goodness-of-fit of the model to the data and then minimizes this function over a domain of parameter values.

ODRPACK does not assume that all measurement errors are in the dependent variables. Rather, it seeks to minimize the weighted sum of orthogonal distances between the model and the data:

$$E_{min} = \min_{\beta,\delta} \left(\sum_{i=1}^{n} \epsilon_i^T w_{\epsilon_i} \epsilon_i + \delta_i^T w_{\delta_i} \delta_i \right), \tag{4}$$

subject to the constraints

$$\epsilon_i = f_i(x_i + \delta_i; \beta) - y_i, i = 1, \ldots, n. \tag{5}$$

In Eq. (4), ϵ_i and δ_i are the vectors of residuals for the dependent and independent variables, respectively, and w_{δ_i} and w_{ϵ_i} are matrices of weighting factors for the errors. The weighting factors are used to translate all observables into a common 'currency' and to express the user's confidence in the reliability of different observations. The solution of problem (4)–(5) consists of $\tilde{\beta}, \tilde{\delta}, \tilde{\epsilon}, E_{min}$, giving the optimal parameter vector, the minimal discrepancies between model and observations, and a scalar measure of the overall goodness-of-fit.

In our problem, all our data points are ordered pairs (x_i, y_i) of scalar quantities, and our objective function is simply

$$E = \sum_{i=1}^{n} w_{\epsilon_i}\epsilon_i^2 + w_{\delta_i}\delta_i^2.$$

In Table 3 we collect all the information necessary to compute E from the model (Eqs. 1–3) and the data (Fig. 2).

ODRPACK uses a trust region Levenberg-Marquardt method with scaling to minimize E (Boggs et al., 1992). In doing so ODRPACK needs to calculate Jacobian matrices (partial derivatives of E with respect to β and δ). ODRPACK can calculate these matrices by finite differences or by a user-supplied routine. Finite differences were used here.

4.2. LSODAR

All solutions of the ODEs (1)–(3) were computed by LSODAR, a variant of LSODE [(Radhakrishnan and Hindmarsh, 1993), (Hindmarsh, 1980), (Hindmarsh, 1983)], which automatically switches between stiff and nonstiff methods and has a root finder. LSODAR starts with a nonstiff method and switches to a stiff method if necessary. LSODAR's root finder is used in this application to find the time lag for MPF activation.

For nonstiff problems LSODAR uses Adams-Moulton (AM) of orders 1 to 12. For stiff problems LSODAR uses backward differentiation formulas (BDF) of orders 1 to 5. With both methods LSODAR varies the step size and order. LSODAR switches from AM to BDF when AM is no longer stable for the problem or cannot meet the accuracy requirements efficiently (Petzold, 1983).

The root finder in LSODAR is based on ZEROIN (Shampine and Allen, 1973). ZEROIN is based on code by Dekker (Dekker, 1969). LSODAR detects a root when the sign changes for the user-defined subroutine GEX.

The tolerances are set to 10^{-12} for both relative and absolute error. A tolerance of 10^{-10} is used when calculating a root for a function of the form $M(t) - M_{root}$, where M_{root} is the value of the function $M(t)$ for which a time, t, is desired.

4.3 Weights

The choice of weights, w_{ϵ_i} and w_{δ_i}, should be guided by several principals. First of all, the weights should convert deviations in x_i and y_i into a common "currency" (E is sometimes called the "cost" or "penalty" function). Secondly, the weights should express the relative reliabilities of the measurements. Ideally, if we have many replicated measurements, we can compute the reliabilities, and hence the weights, from the variance of the measurements. In our case, we don't have this luxury, and we must provide some informal estimate of our confidence in the data. Thirdly, the weights can be used to quantify our assessment of the relative importance of the different experiments.

To these ends, we suggest weights of the form

$$w_{\epsilon_i} = \frac{\alpha_i}{\sigma_{\epsilon_i}^2}, \qquad w_{\delta_i} = \frac{\alpha_i}{\sigma_{\delta_i}^2},$$

where α_i is a dimensionless number that assigns a relative importance to the ith data vector; σ_{ϵ_i} and σ_{δ_i} are constants, carrying the same units as y_i and x_i, respectively, that reflect our relative uncertainties in the measurements (ideally, they should be estimates of the standard deviation of the measurements).

In our case, we choose $\alpha_i = 1$ for all the weights. Our choices of σ_{ϵ_i} and σ_{δ_i} represent a subjective estimate of the standard deviation of each measurement.

In Table 3 we collect all the information necessary to compute E from the model (Eqs. 1–3) and the data (Fig. 2).

5. RESULTS

We have fitted the data in Fig. 2 to two different sets of "optimal" parameter values; the results are reported in Fig. 2 and Table 2. In the first set of optimized parameter values, we fixed the four Michaelis constants at the values chosen by Marlovits et al. (1998). In the second set, we allowed the Michaelis constants to adjust to the data, provided none of them fall below 0.01. Small values for K imply an enzyme with very high affinity for substrate and generate rate laws with sharp "kinks." In our opinion, $K < 0.01$ is biochemically unrealistic, even though the kinks provide moderately better fits to the data. Whether the Ks are fixed or constrained, the optimal values of the other rate constants are in reasonable agreement amongst themselves and compared with the initial estimates of Marlovits et al. (1998) (Table 2). By examining the curves in Fig. 2, one sees clearly that the guesstimates of Marlovits et al. (1998)were pretty good, but ODRPACK was able to find nearby parameter sets that give a better (indeed, optimal) fit of the model to the data.

For both optimization procedures, ODRPACK drove v'_w to very small values, so we fixed $v'_w = 0$ in both cases. In the "fixed K" case, ODRPACK determined that $\rho_d \approx \rho_w$, which gives a simple S-shaped bifurcation curve, as in Fig. 3. For the "constrained K" case, ODRPACK finds an optimal parameter set with $\rho_d \approx \rho_w/10$, in which case the steady-state bifurcation curve (Fig. 3) is double-S-shaped. This effect can be seen in Fig. 2(J), at low cyclin concentrations, where there appear to be two jumps in MPF activity. The experimental data is not good enough to distinguish between these two possibilities. For the sake of simplicity, we prefer the "fixed K" parameter values.

To ensure that ODRPACK found a local minimum of the objective function, we calculated $E(\beta)$ in a neighborhood of β^0, where $\beta^0 = \{p_1^0, p_2^0, \ldots, p_8^0\}$ is the set of optimal parameter values. (For fixed K, there are eight parameters to be optimized: the seven adjustable rate constants in Table 2 plus the dilution factor, μ, as described in footnote (3) to Table 3.) The evaluations were made on a regular grid of points at $0.975p_i^0$, $1.0p_i^0$, and $1.025p_i^0$ in each of the eight directions. All $6,561$ evaluations of E satisfied $E(\beta) > E(\beta^0)$, confirming that ODRPACK had indeed found a local minimum of the objective function.

In addition, we fitted these $6,561$ values of E to a function of the form

$$\tilde{E}(\beta) = E(\beta^0) + \sum_{i,j=1}^{8} a_{ij} \left(\frac{p_i - p_i^0}{p_i^0} \right) \left(\frac{p_j - p_j^0}{p_j^0} \right).$$

The matrix of coefficients, $A = [a_{ij}]$, is symmetric and, hence, can be diagonalized by an orthogonal matrix Q; furthermore, all the eigenvalues of A are real (Gantmacher, 1977). That is to say, $Q^T A Q = \Lambda = diag(\lambda_1, \ldots, \lambda_8)$, where $Q^T Q = I$, $\lambda_1, \ldots, \lambda_8$ are real numbers, and the columns of Q (call them q_i) are the eigenvectors of A. With this information, we can estimate the deviations of E from $E(\beta^0)$ as follows. Let π be a vector whose components are $\pi_i = (p_i - p_i^0)/p_i^0$, $i = 1, \ldots, 8$. Then

$$\tilde{E}(\beta) - E(\beta^0) = \pi^T A \pi = \pi^T Q Q^T A Q Q^T \pi = v^T \Lambda v,$$

where $v = Q^T\pi$. Hence, the eigenvalues and eigenvectors of A give us useful information about the shape of E in the neighborhood of $E(\beta^0)$ (provided, of course, that $\tilde{E}$ is a good approximation to E). In our case, the eigenvalues and eigenvectors of A are reported in Table 4. Because all the eigenvalues are positive, $\tilde{E}$ (considered as a function of π_is) is an eight-dimensional bowl with a local minimum at the origin ($\pi_i = 0$ for all i). Furthermore, the bowl is very flat (i.e., quality of the fit is not sensitive to modest changes in parameter values), in the following sense. $\tilde{E}$ changes most rapidly in the direction of the first eigenvector, because $\lambda_1 = 908.7$ is the largest eigenvalue. For a 2.5% change in parameter values in the direction of q_1, we estimate that $\tilde{E} - E^0 = 0.57$ (Fig. 4), where E^0 is the error at β^0. Since $E^0 = 9.58$, this is only a 6% increase in error. If we dare to extrapolate beyond the data set, then a 4% change in parameter values (in the direction of q_1) would lead to only a 15% increase in error. Hence, we conclude that ODRPACK has indeed found a robust, locally optimal parameter set for this problem.

Similar results were obtained for the "constrained K" case.

6. DISCUSSION

Computational models of cell growth and division involve digital representation of a complex network of biochemical reactions within cells. These reactions can be described by a system of nonlinear ordinary differential equations, according to the principles of biochemical kinetics. Rate constants and binding constants enter as parameters in the differential equations, and must be estimated by fitting solutions of the equations to experimental data.

ODRPACK, based on the orthogonal distance between experimental data and the model, is used for the nonlinear regression to estimate the unknown rate constants (ODE parameters). The ability of this algorithm to arbitrarily weight data values, and to treat both the abscissa and ordinates as uncertain, is crucial, given the sparsity and uncertainty of available biological data.

The complete calculation is expensive, because the ODEs are stiff, and must be solved numerous times for the nonlinear regression. Also, because of local minima, the nonlinear regression must be done from many starting points to adequately explore the parameter space. There are potential sources for parallelism in multiple starting points for regression and in the multiple experiments being simulated.

To study realistic models of cell cycle control, more components must be added to the model, and other measurable phenomena incorporated in the cost function. As the modeling fidelity is increased, the mathematical and computational complexities of the problem grow rapidly. Efficient and accurate tools for parameter estimation will be needed to build computational models of the complex control networks operating within cells, which is one of the main goals of bioinformatics in the postgenomic era.

ACKNOWLEDGMENTS

The work reported herein was sponsored by the National Science Foundation (NSF) Biocomplexity Program, Grant MCB-0083315, and by the Defense Advanced Research Projects Agency (DARPA) and Air Force Research Laboratory (AFRL), Air Force Material Command, USAF, under agreement number F30602-02-0572. The U.S. Government is authorized to reproduce and distribute reprints for Governmental purposes notwithstanding any copyright annotation thereon. The views and conclusions contained herein are those of the authors and should not be interpreted as necessarily representing the official policies or endorsements, either expressed or implied, of NSF, DARPA, AFRL, or the U.S. Government.

REFERENCES

Boggs, P.T., Byrd, R.H., Donaldson, J.R., and Schnabel, R.B. 1989. Algorithm 676 — ODRPACK: Software for Weighted Orthogonal Distance Regression. *ACM Trans. Math. Software 15*. 4, 348–364.

Boggs, P.T., Byrd, R.H., Rogers, J.E., and Schnabel, R.B. 1992. *User's Reference Guide for ODRPACK Version 2.01: Software for Weighted Orthogonal Distance Regression*, Center for Computing and Applied Mathematics, U.S. Department of Commerce, Gaithersburg, MD.

Dekker, T.J. 1969. Finding a zero by means of successive linear interpolation. In Dejon, B., and Henrici, P., eds., *Constructive Aspects of the Fundamental Theorem of Algebra* Wiley-Interscience, London.

Gantmacher, F. R. 1977. *The Theory of Matrices*, Chelsea Publishing Company, New York, NY.

Gear, C.W. 1971. *Numerical Initial Value Problems in Ordinary Differential Equations*, Prentice-Hall, Englewood Cliffs, NJ.

Hindmarsh, A.C. 1980. LSODE and LSODI, Two New Initial Value Ordinary Differential Equation Solvers. *ACM SIGNUM Newsletter 15*. 4, 10–11.

Hindmarsh, A.C. 1983. ODEPACK: A Systematized Collection of ODE Solvers, 55–64. In Stepleman, R.S., et al., eds., *Scientific Computing* North Holland Publishing Co., New York.

Kahaner, D., Moler, C., and Nash, S. 1989. *Numerical Methods and Software*, Prentice-Hall, Inc., Englewood Cliffs, NJ.

Kumagai, A., and Dunphy, W. G.. 1992. *Regulation of the cdc25 Protein during the Cell Cycle in Xenopus Extracts*. Cell.70, 139–151

Kumagai, A., and Dunphy, W. G.. 1995. *Control of the Cdc2/Cyclin B Complex in Xenopus Egg Extracts Arrested at a G2/M Checkpoint with DNA Synthesis Inhibitors*. Mol. Bio. of the Cell.6, 199–213

Marlovits, G., Tyson, C.J., Novak, B., and Tyson, J.J. 1998. Modeling M-phase control in Xenopus oocyte extracts: the surveillance mechanism for unreplicated DNA. *Biophys. Chem.*. 72, 169–184.

Moore, J. 1997. Private Communication, Aug.

Murray, A. and Hunt, T. 1993. *The Cell Cycle*, W. H. Freeman and Company, New York, NY.

Novak, B. and Tyson, J. 1993. Numerical Analysis of a Comprehensive Model of M-phase Control in Xenopus Oocyte Extracts and Intact Embryos. *Journal of Cell Science*. 106, 1153–68.

Petzold, L. 1983. Automatic Selection of Methods for Solving Stiff and Nonstiff Systems of Ordinary Differential Equations. *SIAM Journal on Scientific and Statistical Computing*. 4, 136–148.

Radhakrishnan, K., and Hindmarsh, A.C. 1993. *Description and Use of LSODE, the Livermore Solver for Ordinary Differential Equations*, NASA Reference Publication 1327. Lawrence Livermore National Laboratory, Livermore, CA, Dec.

Shampine, L.F., and Allen, R.C. 1973. *Numerical Computing: An Introduction*, W. B. Saunders Company, Philadelphia, PA.

Shampine, L.F., and Gordon, M.K. 1975. *Computer Solution of Ordinary Differential Equations, The Initial Value Problem*, W. H. Freeman, San Francisco, CA.

Solomon, M. J., Glotzer, M., Lee, T. H., Philippe, M., and Kirschner, M. W. 1990. Cyclin Activation of P34cdc2. *Cell*. 63, 1013–1024.

Tang, Z., Coleman, T. R., and Dunphy, W. G.. 1993. *Two distinct mechanisms for negative regulation of the Wee1 protein kinase*. EMBO J..12, 9:3427–36

Tyson, J. J., Chen, K., and Novak, B. 2001. Network Dynamics and Cell Physiology. *Nature Reviews Molecular Cell Biology*. 2, 908–16.

Tyson, J. J., Novak, B., Chen, K., and Val, J. 1995. Checkpoints in the cell cycle from a modeler's perspective. *Progress in Cell Cycle Research*. 1, 1–8.

Wei, S., Moore, J., Chen, K., Lassaletta, A. D., Yi, C. S., Tyson, J. J., and Sible, J. C. 2002. Hysteresis Drives Cell-Cycle Transitions in *Xenopus Laevis* Egg Extracts. submitted for publication.

APPENDIX A: Pseudocode for TIMELAG

TIMELAG takes as parameters C_T and a. C_T is the total cyclin concentration and a is 0 if MPF is initially inactive and 1 if MPF is initially active.

subroutine TIMELAG
if $C_T \leq 0$ **then**
  TIMELAG $= -1440 * C_T + 2880$;
  return;
endif
M_{inf} = asymptotic concentration of active MPF, retrieved from a call to LSODAR;
Comment: Check if MPF changes from active to inactive or vice versa. If it does not change its activity then return.
if ($M_{inf} > C_T/2$ **and** $a = 1$) **or** ($M_{inf} < C_T/2$ **and** $a = 0$) **then**
  TIMELAG $= -1440 * C_T + 2880$;
  return
endif
Comment: Use the root finder in LSODAR to find the timelag.
if $a = 1$ **then**
  TIMELAG = time where MPF concentration is $(C_T - M_{inf})/2 + M_{inf}$
else
  TIMELAG = time where MPF concentration is $M_{inf}/2$
endif
return
end subroutine TIMELAG

APPENDIX B: Pseudocode for THRESHOLD

The THRESHOLD function calculates the threshold for MPF activation or inactivation for a given set of rate constants β. If the first parameter, a, to THRESHOLD is 1 then MPF is initially active and the inactivation threshold is calculated. If the first parameter to THRESHOLD is 0 then MPF is initially inactive and the activation threshold is calculated. The estimate for the threshold is returned in h.

subroutine THRESHOLD
  $B := 0.001$; Initialize the lower bound for the threshold. The initial value of B may not be a lower bound. A more realistic lower bound will be found later, if B is not a lower bound.
  $C := 1$; Initialize the upper bound for the threshold. The initial value of C may not be an upper bound. A more realistic upper bound will be found later, if C is not an upper bound.
  $e_{tol} := 10^{-10}$; Define the error tolerance for calculating the threshold.

Find the lower bound on the threshold.

while (($a = 0$ **and** TIMELAG$(a, \beta, b) < 1440$) **or** ($a = 1$ **and** TIMELAG$(a, \beta, b) \geq 1440$)) **and** ($b > e_{tol}$) **do**

$b := b/2$;

enddo

if $b \leq e_{tol}$ **then**

$h := b$;

return;

endif

Find the upper bound on the threshold.

while (($a = 0$ **and** TIMELAG$(a, \beta, c) \geq 1440$) **or** ($a = 1$ **and** TIMELAG$(a, \beta, c) < 1440$)) **and** ($c < 1/e_{tol}$) **do**

$c := c * 2$;

enddo

if $c \geq 1/e_{tol}$ **then**

$h := c$;

return;

endif

while $(c - b)/b > e_{tol}$ **do**

$next = (c + b)/2$; Bisect the interval.

if ($a = 0$ **and** TIMELAG$(a, \beta, next) \geq 1440$) **or** ($a = 1$ **and** TIMELAG$(a, \beta, next) < 1440$) **then**

$b := next$;

else

$c := next$;

endif

enddo

$h := b$;

end subroutine THRESHOLD

Table 1. Estimated parameter values (Marlovits et al., 1998). μ = dilution factor (see text).

Unscaled Parameters		**Scaled Parameters**	
Name	**Value**	**Name**	**Value**
$\hat{v}'_d$	0.017 $\mathrm{AU_d^{-1}min^{-1}}$	$v'_d = \mu\hat{v}'_d$[totalCdc25]	0.017 $\mathrm{min^{-1}}$
$\hat{v}''_d$	0.17 $\mathrm{AU_d^{-1}min^{-1}}$	$v''_d = \mu\hat{v}''_d$[totalCdc25]	0.17 $\mathrm{min^{-1}}$
$\hat{v}'_w$	0.01 $\mathrm{AU_w^{-1}min^{-1}}$	$v'_w = \mu\hat{v}'_w$[totalWee1]	0.01 $\mathrm{min^{-1}}$
$\hat{v}''_w$	1.0 $\mathrm{AU_w^{-1}min^{-1}}$	$v''_w = \mu\hat{v}''_w$[totalWee1]	1.0 $\mathrm{min^{-1}}$
$\hat{v}_d$	0.02 $\mathrm{AU_d\ nM^{-1}min^{-1}}$	$v_d = \hat{v}_d$[totalCdk1]/[totalCdc25]	2.0 $\mathrm{min^{-1}}$
$\hat{v}_w$	0.02 $\mathrm{AU_w\ nM^{-1}min^{-1}}$	$v_w = \hat{v}_w$[totalCdk1]/[totalWee1]	2.0 $\mathrm{min^{-1}}$
$\hat{v}_{dr}$	0.1 $\mathrm{AU_d\ AU_p^{-1}min^{-1}}$	$\rho_d = (\hat{v}_{dr}/\hat{v}_d)$[PPase]/[totalCdk1]	0.05
$\hat{v}_{wr}$	0.1 $\mathrm{AU_w\ AU_p^{-1}min^{-1}}$	$\rho_w = (\hat{v}_{wr}/\hat{v}_w)$[PPase]/[totalCdk1]	0.05
$\hat{K}_{md}$	0.1 $\mathrm{AU_d}$	$K_{md} = \hat{K}_{md}/(\mu$[totalCdc25])	0.1
$\hat{K}_{mdr}$	1.0 $\mathrm{AU_d}$	$K_{mdr} = \hat{K}_{mdr}/(\mu$[totalCdc25])	1.0
$\hat{K}_{mw}$	0.1 $\mathrm{AU_w}$	$K_{mw} = \hat{K}_{mw}/(\mu$[totalWee1])	0.1
$\hat{K}_{mwr}$	1.0 $\mathrm{AU_w}$	$K_{mwr} = \hat{K}_{mwr}/(\mu$[totalWee1])	1.0
[totalCdk1]	100 nM		
[totalCdc25]	1 $\mathrm{AU_d}$		
[totalWee1]	1 $\mathrm{AU_w}$		
[PPase]	1 $\mathrm{AU_p}$		

Table 2. Initial and final estimated parameter values. The initial values come from Marlovits et al. (1998), and the final values are our optimal parameter set for fitting the data in Fig. 2. We present two "optimal" parameter sets: one with fixed Ks (the Michaelis constants are fixed at the values chosen by Marlovits et al. (1998)), and one with constrained Ks (the Michaelis constants are allowed to vary, but they may not fall below 0.01). The last row reports the value of the error function E for each of the three parameter sets.

Rate Constant	Initial	Fixed Ks	Constrained Ks
v'_d	0.017	0.0198	0.0148
v''_d	0.17	0.181	0.195
ρ_d	0.05	0.0537	0.0044
v'_w	0.01	0.00	0.00
v''_w	1.0	1.256	1.213
ρ_w	0.05	0.0303	0.036
K_{md}	0.1	0.1	0.01
K_{mdr}	1.0	1.0	0.01
K_{mw}	0.1	0.1	0.01
K_{mwr}	1.0	1.0	0.072
v_d	2.0	2.563	10.7
v_w	2.0	8.775	2.344
$E(\beta)$	68.9	9.58	5.02

Table 3. Parameter values, initial conditions, and weights assigned to each experiment in Fig. 2.

		Data		Weights		Params		Initial Conditions		
Exp	**Notes**	x	y	w_δ	w_ϵ	μ	C_T	M	D	W
A	(1)	t	$L(t)$			1	0	0	0	1
		2	1	1	100					
		4	1	1	100					
		16	1	1	100					
B	(1)	t	$L(t)$			1	1	1	1	0
		4	0	1	100					
		16	0	1	100					
C	(2)	t	$L_p(t)$			1	0	0	0	1
		2	1	1	100					
		4	1	1	100					
		8	0.85	1	100					
D	(2)	t	$L_p(t)$			1	1	1	1	0
		2	0.75	1	100					
		4	0.51	1	100					
		8	0.21	1	100					
E		t	$D(t)$			0.83	0.25	0.25	0	0
		1.25	0.8	1	100					
		2.5	0.9	1	100					
		5	1	1	100					
		10	1	1	100					
F		t	$D(t)$			0.83	0	0	1	0
		5	0.75	1	100					
		10	0.5	1	100					
		20	0.1	1	100					
		40	0	1	100					
G		t	$W(t)$			0.67	0.254	0.254	1	1
		2	0.5	1	100					
		5	0	1	100					
		7	0	1	100					
		10	0	1	100					
H		t	$W(t)$			0.67	0	0	1	0
		7.5	0.5	1	100					
		15	1	1	100					

Table 3. Continued.

		Data		Weights		Params		Initial Conditions		
Exp	**Notes**	x	y	w_δ	w_ϵ	μ	C_T	M	D	W
I	(3,4)	C_T	Lag			-	-	0	0	1
		0.2	45	2500	0.01					
		0.25	40	2500	0.01					
		0.3	30	2500	0.01					
		0.5	20	2500	0.01					
J	(3,5)	-	Thresh			-	-			
		-	0.18	-	2500			0	0	1
		-	3	-	11			1	1	0

Notes

(1) For experiments A and B, Eqs (1)–(3) are supplemented by

$$\frac{dL}{dt} = (v'_w(1-W) + v''_w W)(1-L), \quad L(0) = 0$$

(2) For experiments C and D, Eqs (1)–(3) are supplemented by

$$\frac{dL_p}{dt} = (v'_d(1-D) + v''_d D)L_p, \quad L_p(0) = 1$$

(3) For experiments I and J, μ is considered to be an adjustable parameter. Initially, it is set to 1, and it reaches an optimal value of 1.015. This means that Moore's extracts have effectively the same dilution as Dunphy's.

(4) See Appendix A for a description of how to compute lag times for MPF activation.

(5) See Appendix B for a description of how to compute thresholds for MPF activation and inactivation.

Table 4. The eigenvalues and eigenvectors of A (see text).

i	λ_i	q_{i1} (v'_d)	q_{i2} (v''_d)	q_{i3} (ρ_d)	q_{i4} (v''_w)	q_{i5} (ρ_w)	q_{i6} (v_d)	q_{i7} (v_w)	q_{i8} (μ)
1	908.7	0.3305	0.3779	−0.328	−0.653	−0.192	0.0491	0.0336	−0.415
2	168.0	0.0410	0.1622	0.5665	−0.118	−0.371	0.6804	−0.094	0.1641
3	135.1	0.1371	−0.049	0.2365	−0.098	0.7422	0.3153	0.4535	−0.238
4	60.0	−0.049	0.5087	−0.114	−0.024	−0.039	−0.112	0.5868	0.6052
5	26.3	0.1775	−0.749	−0.153	−0.387	−0.199	0.0837	0.2954	0.3156
6	10.8	0.8153	0.0691	0.0483	0.1061	0.2272	−0.099	−0.353	0.3606
7	6.3	0.0489	0.0092	−0.669	0.4024	0.0066	0.6215	−0.012	0.0140
8	2.8	0.4112	−0.057	0.1649	0.4754	−0.425	−0.138	0.4765	−0.383

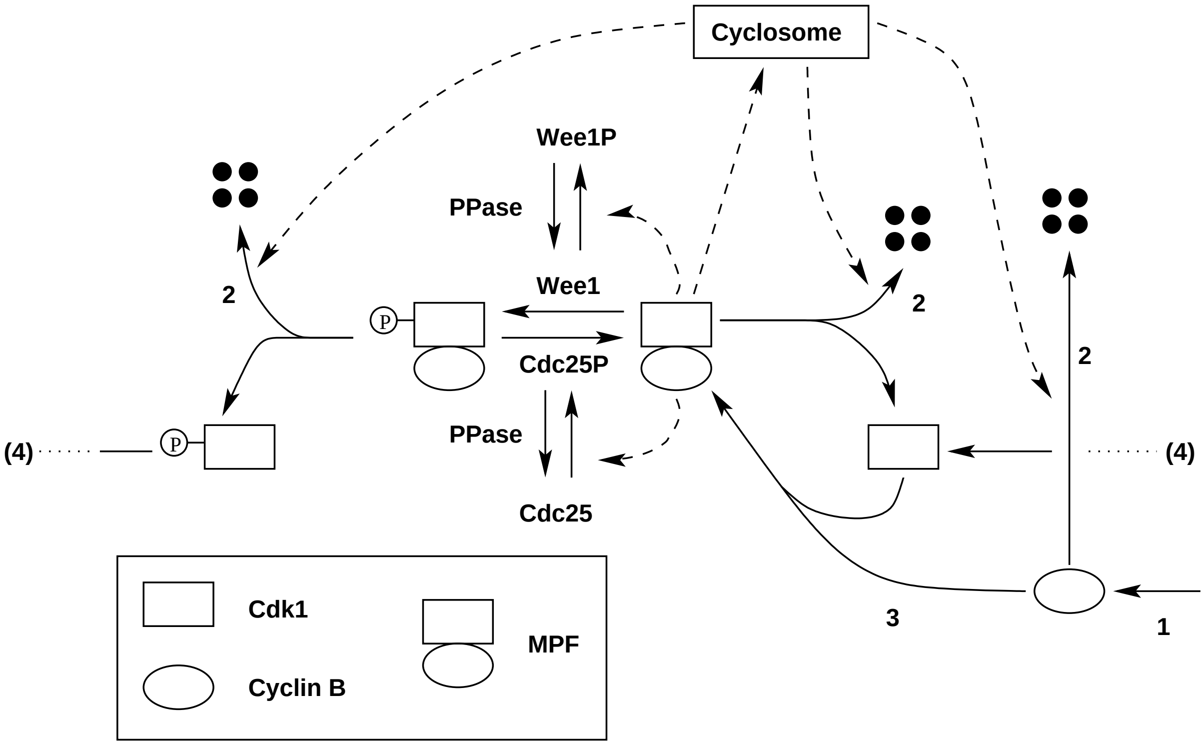

FIG. 1. The biochemical control system for MPF activation in frog egg extracts. MPF = mitosis-promoting factor = dimer of a cyclin-dependent kinase, Cdk1 (rectangle), and a B-type cyclin (oval). Rising MPF activity drives an extract through DNA synthesis, nuclear envelope breakdown, chromosome condensation, and alignment of replicated chromosomes on the mitotic spindle. Falling MPF activity allows for sister chromatid separation, nuclear reassembly, and licensing of DNA for another round of replication. Cycles of MPF activation and inactivation are driven by phases of cyclin synthesis and degradation, and by phases of Cdk1 phosphorylation (by Wee1) and dephosphorylation (by Cdc25). The newly fertilized egg has a large supply of Cdk1, the enzymes Wee1 and Cdc25, and cyclosomes (the protein complexes that promote cyclin B degradation in the steps labeled 2). The only missing component is Cyclin B. As cyclin is synthesized (step 1), it combines rapidly (step 3) with Cdk1 monomers to form active MPF dimers. The active dimers, however, are rapidly phosphorylated by Wee1 to a less active form. During this phase of the cycle, cyclins are relatively stable because the cyclosome is inactive. For the extract to enter mitosis, the inhibitory phosphate groups must be removed from Cdk1 by Cdc25. Activation of MPF is an autocatalytic process because active MPF activates Cdc25 and inhibits Wee1 (PPase is a phosphatase that opposes MPF in these reactions). As MPF activity rises, nuclei are driven into mitosis and cyclosomes are activated. The cyclosomes promote rapid cyclin degradation, which destroys MPF activity and allows nuclei to finish mitosis and prepare for a new round of DNA replication.

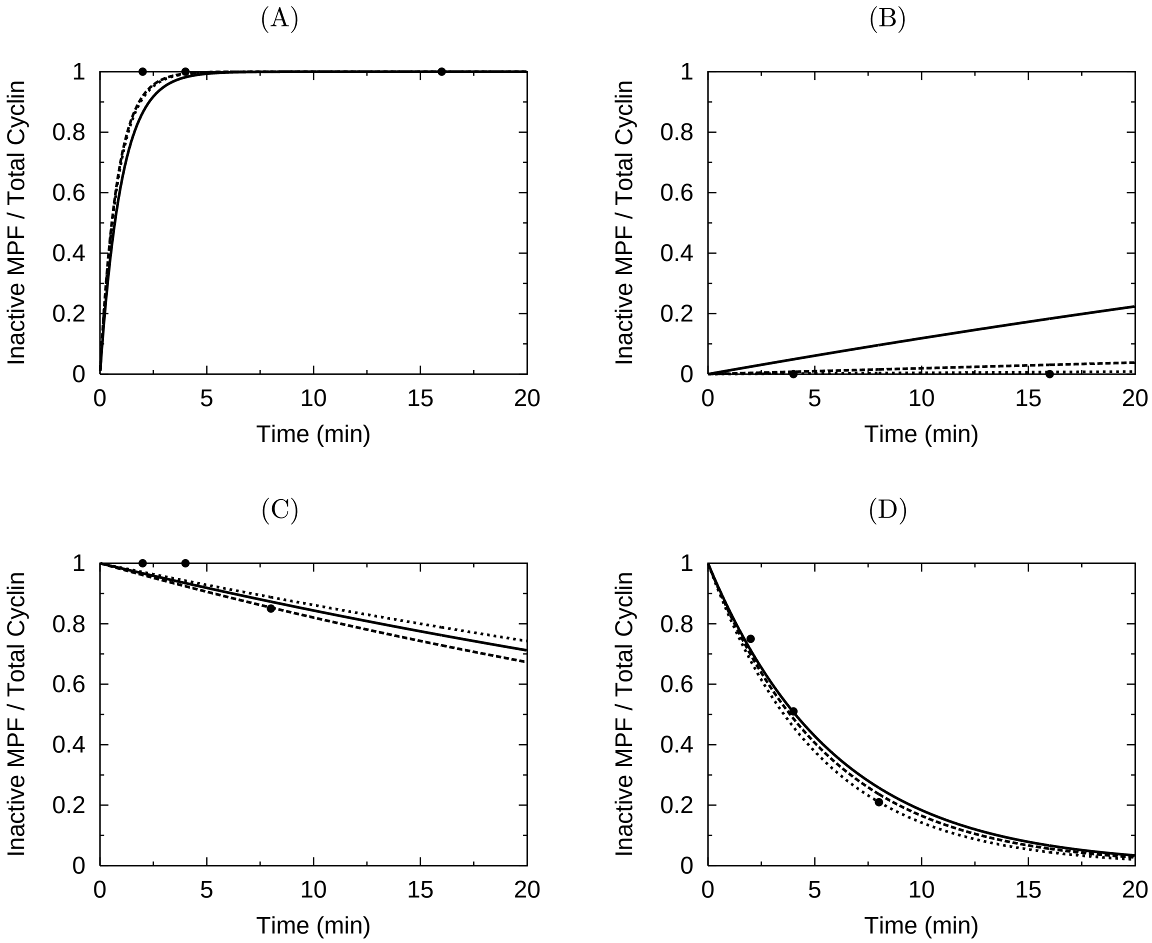

FIG. 2. Experimental data (•) used for parameter estimation, simulations (····· and ----) generated by the optimal parameters with Ks fixed and constrained, respectively, and simulations (——) generated by the Marlovits et al. (1998) parameters. (A) Kumagai and Dunphy (1995), Fig. 3C. Phosphorylation of MPF during interphase, when Wee1 is more active. (B) Kumagai and Dunphy (1995), Fig. 3C. Phosphorylation of MPF during mitosis, when Wee1 is less active. (C) Kumagai and Dunphy (1995), Fig. 4B. Dephosphorylation of preMPF during interphase, when Cdc25 is less active. (D) Kumagai and Dunphy (1995), Fig. 4B. Dephosphorylation of preMPF during mitosis, when Cdc25 is more active. (E) Kumagai and Dunphy (1992), Fig. 10A. Phosphorylation of Cdc25 during mitosis, when MPF is more active. (F) Kumagai and Dunphy (1992), Fig. 10A. Dephosphorylation of Cdc25 during interphase. (G) Tang et al. (1993), Fig. 2. Phosphorylation of Wee1 during mitosis, when MPF is more active. (H) Tang et al. (1993), remark in text (p. 3430). Dephosphorylation of Wee1 during interphase. (I) Moore (1997). Time lag for MPF activation. (J) Moore (1997). Thresholds for MPF activation (↑) and inactivation (↓).

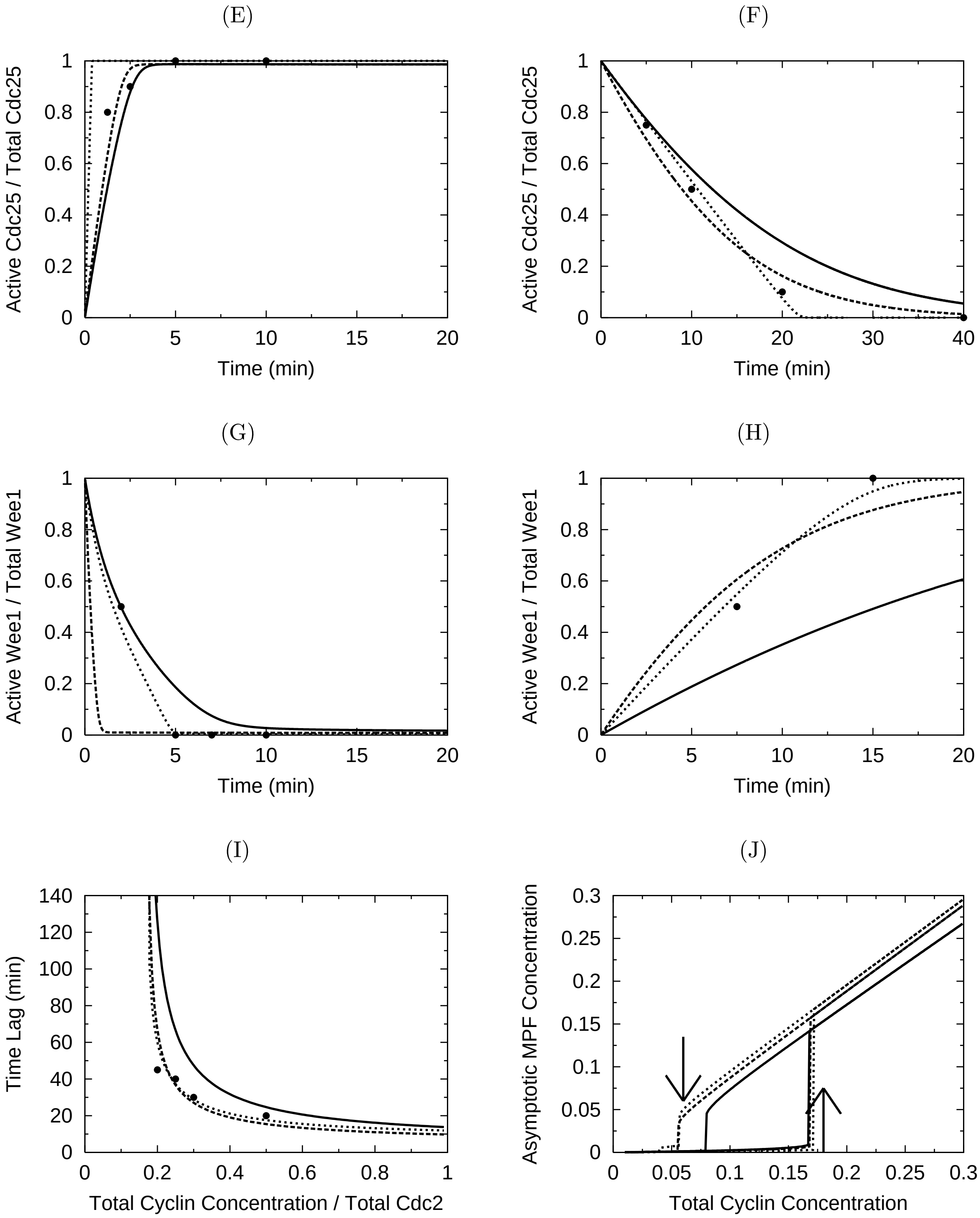

FIG. 2. Continued.

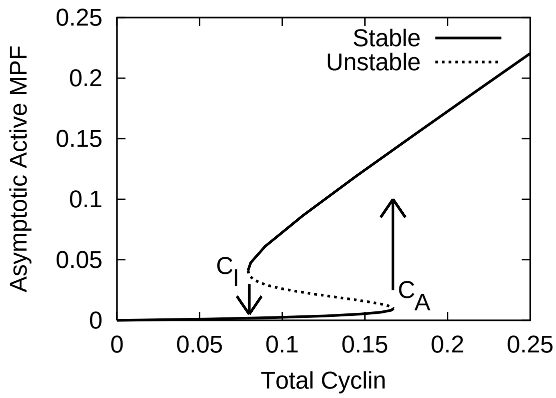

FIG. 3. Steady-state MPF activity versus total cyclin concentration. This S-shaped curve was computed from Eqs. (1)–(3) by setting all time derivatives equal to 0 and solving the resulting nonlinear algebraic equations for M as a function of C_T. All other parameters in the equations are given the values estimated by Marlovits et al. (1998), see Table 1. C_A = activation threshold, C_I = inactivation threshold.

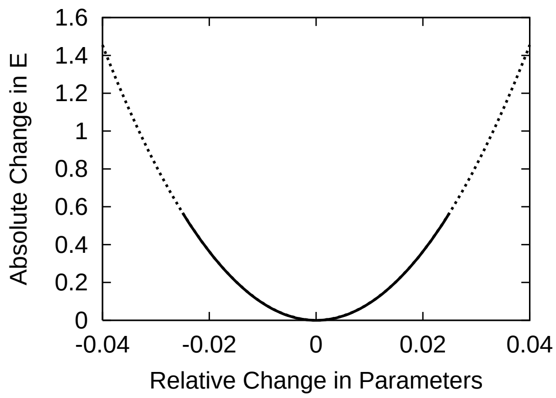

FIG. 4. Absolute changes in the error function with respect to relative changes in the parameters in the direction of q_1. q_1 is the eigenvector corresponding the the maximum eigenvalue. Therefore, this plot represents the maximum change in the error function with respect to the parameters in the neighborhood of the optimal parameters. The solid line (—) represents the range of the fitted data. The dotted line (.....) represents an extrapolation of the quadratic fit. The error function is plotted for the "fixed K" case ($\lambda_1 = 909$). The curve is almost the same for the "constrained K" case ($\lambda_1 = 1168$).